Journal of Molecular Structure 1243 (2021) 130863

Contents lists available at ScienceDirect

Journal of Molecular Structure

journal homepage: www.elsevier.com/locate/molstr

2-(2-Amino-6-methylpyrimidin-4-yl)-4-arylmethylidene-5-methyl-2,4-dihydro-3*H*-pyrazol-3-ones: Design, synthesis, structure, *in vitro* anti-tubercular activity, and molecular docking study

Andrei V. Erkin[a,*], Aleksandra V. Yurieva[a], Oleg S. Yuzikhin[b,c], Vladislav V. Gurzhiy[d], Viktor I. Krutikov[a]

[a] Department of Chemistry and Technology of Synthetic Biologically Active Compounds, Saint Petersburg State Institute of Technology (Technical University), 26 Moskovskiy avenue, 190013 Saint Petersburg, Russia
[b] Laboratory of Microbiological Plant Protection, All-Russian Institute of Plant Protection, 3 Podbel'skiy highway, 196608 Saint Petersburg, Pushkin-8, Russia
[c] Laboratory of Rhizosphere Microflora, All-Russian Research Institute of Agricultural Microbiology, 3 Podbel'skiy highway, 196608, Saint Petersburg, Pushkin-8, Russia
[d] Department of Crystallography, Institute of Earth Sciences, Saint Petersburg State University, 7-9 Universitetskaya embankment, 199034 Saint Petersburg, Russia

ARTICLE INFO

Article history:
Received 14 March 2021
Revised 8 May 2021
Accepted 8 June 2021
Available online 11 June 2021

Keywords:
2*H*-Pyrazol-3-ols
Aromatic aldehydes
Knoevenagel condensation
Structure
Anti-tubercular activity
Molecular docking

ABSTRACT

A series of 2-(2-amino-6-methylpyrimidin-4-yl)-4-arylmethylidene-2,4-dihydro-3*H*-pyrazol-3-ones **6a-f** was *in silico* predicted to display moderate anti-tubercular activity. To obtain these compounds, the Knoevenagel condensation of the corresponding pyrazol-3-ol **10** with aromatic aldehydes was performed. It was found that arylidenepyrazolones **6b, 6d** and **6e** bearing 4-diethylamino (**6b**), 3,4-dimethoxy (**6d**) and 4-hydroxy-3-methoxy (**6e**) substituents on the arylidene pendant did possess activity against *Mycobacterium tuberculosis* H37Rv. Their minimal inhibitory concentrations (MICs = 0.07-0.14 mmol/L) were comparable with MIC value for isoniazid (0.01 mmol/L) used as the reference drug. In accordance with a molecular docking study, a plausible mode of action of arylidenepyrazolones **6b, 6d** and **6e** was the inhibition of UDP-galactopyranose mutase responsible for the biosynthesis of arabinogalactan, one of the important components of the mycobacterial cell wall. The above results indicated that compounds **6b, 6d** and **6e** might serve as promising hits in further search for anti-tubercular agents based thereon.

© 2021 Elsevier B.V. All rights reserved.

1. Introduction

Pyrimidines bearing a pyrazole moiety at one of the even-numbered positions of the ring represent N-pyrazolylpyrimidines **1**, an important class of hybrid heterocycles with diverse biological properties. Compounds **1** possess anti-tubercular [1], anti-inflammatory [2], and cytoprotective antiulcer [3] activities. Moreover, 3-methyl-5-methoxy-1-(6-methyl-4-methoxypyrimidin-2-yl)-1*H*-pyrazole (**2**), better known as mepirizole, is clinically used as an oral non-steroidal anti-inflammatory drug for muscle and joint pain [4] (Fig. 1). N-Pyrazolylpyrimidines **1** are of certain interest as antioxidant and anti-inflammatory agents [5], inhibitors of human dihydroorotate dehydrogenase [6], Syk kinase [7] and cyclin-dependent kinase 2 [8], antibacterial and antimalarial agents [9], and pesticides [10]. Among compounds **1**, a promising low-molecular-weight hit against *Staphylococcus aureus* [11] and an inhibitor of human solute carrier protein SLC11A2 [12] have also been found.

The mepirizole **2** precursor is tautomeric methylene ketone **3** [13], which, when reacting with aldehydes, gives the Knoevenagel condensation products **4** [14–17] (Fig. 1). These compounds have been prepared mainly as methine dyes, so there appears to be no available data on their biological activity. Nevertheless, arylidene derivatives **4** (R = Ar) were *a priori* asserted to be less toxic than those of edaravone, 5-methyl-2-phenyl-2,4-dihydro-3*H*-pyrazol-3-one [18]. As a continuation of our work in the field of synthesis and biological screening of compounds **4** (R = Ar) [19], we have fulfilled the present research[1] on their analogues with modified pyrimidine moiety.

* Corresponding author.
E-mail address: anerkin@yandex.ru (A.V. Erkin).

[1] This research did not receive any specific grant from funding agencies in the public, commercial, or not-for-profit sectors

https://doi.org/10.1016/j.molstruc.2021.130863
0022-2860/© 2021 Elsevier B.V. All rights reserved.

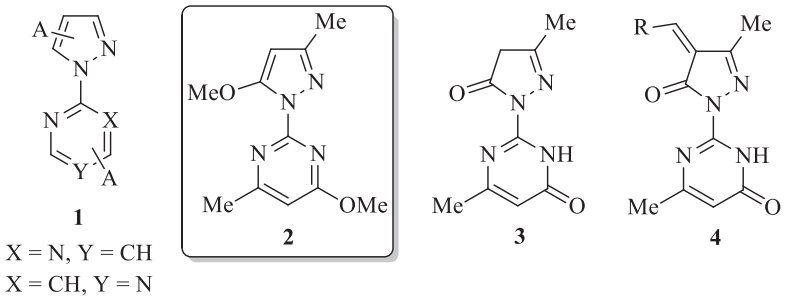

Fig. 1. Structures of N-pyrazolylpyrimidines 1-4.

2. Materials and methods

2.1. Chemistry

All required chemicals and solvents were purchased from commercial sources (Sigma-Aldrich, Fluka and Merck) and used without further purification, except phosphorus oxychloride and ethyl acetoacetate. Reaction progress was monitored by thin layer chromatography (TLC) using pre-coated aluminum sheets plates 60 F254 (Merck Corp., USA) in a *n*-BuOH/AcOH/H_2O (1:1:1, v/v/v) solvent system. The spots were detected by exposure to a UV lamp at 254 nm.

Melting points were determined with PTP block (Khimlabpribor Ltd, Russia). The ^{1}H (400 MHz) and ^{13}C (100 MHz) NMR spectra as well as ^{13}C NMR DEPT-135, {^{1}H-^{13}C}HMQC and {^{1}H-^{13}C}HMBC spectra were registered on a Bruker Avance III HD 400 NanoBay spectrometer (Bruker BioSpin, GmbH, Germany) in DMSO-d_6 and in $CDCl_3$, the signals of residual protons of the solvents served as internal references. The chemical shifts are expressed in the δ (ppm). The coupling constants (J) are given in Hertz (Hz). Spin multiples are given as s (singlet), d (doublet), dd (doublets of doublets), t (triplet), q (quartet), and bs (broad singlet). IR spectra were recorded on a Shimadzu IR Tracer 100 spectrophotometer (Shimadzu Corp., Japan) from KBr pellets. LC-HRMS analysis was performed using Waters BEH-C18 column (100 × 3.0 mm, 3.5 μm) and a 6538 Q-TOF mass spectrometer equipped with an ESI interface (Agilent Technologies, Santa Clara, CA, USA). LC: ambient temperature, injection volume 1-5 µL, the rate flow 0.15 mL/min. The mobile phases were water-acetonitrile 95:5 + 0.1% formic acid (A) and acetonitrile-water 90:10 + 0.1% formic acid (B). The gradient was as follows: 0-1 min 0% B; 1-13 min 0% → 90% B; 13-20 min, 90% B; and 20-25 min, 90% → 0% B. HRMS (positive ion mode): drying gas (N_2) flow rate 7.0 L/min; drying gas temperature 350°C; nebulizer pressure 30 psig; fragmentor voltage 175 V; capillary voltage 3500 V; octapoleRFPeak voltage 750 V, and skimmer voltage 65 V. All the acquisitions and analyses of data were controlled by MassHunter software B.05.00 (Agilent Technologies).

2.2. Single crystal X-ray diffraction study

The single-crystal XRD analysis was performed on the Rigaku Oxford Diffraction XtaLAB HyPix-3000 diffractometer and the diffraction data have been collected using monochromated microfocused Cu$K\alpha$ radiation. Data were integrated and corrected for background, Lorentz, and polarization effects. An empirical absorption correction based on spherical harmonics implemented in the SCALE3 ABSPACK algorithm was applied in *CrysAlisPro* program [20]. The unit-cell parameters ([*P*-1, a = 7.2765(4), b = 9.6556(5), c = 13.2376(5) Å, α = 71.290(4), β = 75.740(5), γ = 85.101(5) °, V = 852.04(8) Å^3, Z = 2, R_1 = 7.9%], Table S1) were refined by the least-squares techniques. The structure was solved by dual-space algorithm and refined using the *SHELX* programs [21, 22] incorporated in the *OLEX2* program package [23]. The final model included coordinates and anisotropic displacement parameters for all non-H atoms. Selected interatomic bonds and angles are listed in Table S2. The carbon and nitrogen-bound H atoms were placed in calculated positions and were included in the refinement in the 'riding' model approximation, U_{iso}(H) set to 1.5U_{eq}(C) and C–H 0.96 Å for the CH_3 groups, U_{iso}(H) set to 1.2U_{eq}(C) and C–H 0.93 Å for the CH groups, and U_{iso}(H) set to 1.2U_{eq}(N) and N–H 0.86 Å for the NH_2 group. The H atoms of H_2O molecules were localized from difference Fourier maps and were included in the refinement with U_{iso}(H) set to 1.5U_{eq}(O) and O–H restrained to 0.85 Å. CCDC 2013983 contains the supplementary crystallographic data for this paper. These data can be obtained free of charge via http://www.ccdc.cam.ac.uk/conts/retrieving.html.

2.3. Synthesis

2.3.1. General procedure for the synthesis of 2-(2-amino-6-methylpyrimidin-4-yl)-4-aryl-methylidene-5-methyl-2,4-dihydro-3H-pyrazol-3-ones (**6a-f**)

A mixture of pyrazol-3-ol **10** (0.5 g, 2.4 mmol) and 2.4 mmol of appropriate aromatic aldehyde in acetic acid (10 mL) was heated at 80°C for 1 h. After cooling, compounds **6a, 6c-6f** were isolated as colored precipitates by filtration, compound **6b** was isolated as a colored solid upon evaporation of the solvent to dryness. Purification of compounds **6a-f** thus obtained was carried out as follows. Compounds **6a** and **6b** were recrystallized from H_2O-AcOH (5:3, v/v) and from EtOH-DMF (2:1, v/v), respectively; compounds **6d** and **6f** were recrystallized from H_2O-AcOH (1:2, v/v); compounds **6c** and **6e** were briefly heated with EtOH (10 mL) and H_2O (10 mL), respectively. After washing with a small amount of warm water, compounds **6a-f** were dried at 70°C to a constant weight.

2.3.2. Synthesis of (Z)-2-(2-amino-6-methylpyrimidin-4-yl)-4-[(4-dimethylaminophenyl)-methylidene]-5-methyl-2,4-dihydro-3H-pyrazol-3-one (**6a**)

Yield[2]: 45%; Mp: > 255°C (dec.). ^{1}H NMR, δ (ppm) (DMSO-d_6): 2.27 (s, 6H, Me), 3.14 (s, 6H, MeN), 6.45 (s, 2H, NH_2), 6.79 (t, 2H, ArH, ^3J = 8.7 Hz), 7.24 [s, 1H, C(5)H], 7.45 (s, 1H, H$^{\beta}$), 8.54 (d, 2H, ArH, ^3J = 6.5 Hz); ^{13}C NMR, δ (ppm) (DMSO-d_6): 13.71 (Me, pyrazole ring), 24.31 (Me, pyrimidine ring), 39.97 (MeN), 97.36 [C(5)], 111.7 [C(3'')], 118.3 [C(4')], 121.5 [C(1'')], 137.9 [C(2'')], 148.8 (C$^{\beta}$), 152.8 [C(5')], 154.4 [C(4'')], 157.2, 163.7, 163.9 [C(3')], 168.4 [C(6)]. ^{13}C NMR DEPT-135, δ (ppm) (DMSO-d_6): 13.55, 24.32, ~ 40, 97.59, 111.9, 138.1, 148.8. IR, ν_{max} (cm^{-1}) (KBr): 1672 ($\nu_{C=O}$), 1623

[2] The yield optimization is currently underway and results thereof will be published elsewhere

($\nu_{C=N}$), 1549 ($\nu_{C=C}$). LC, rt (min): 13.63-13.73. HRMS (ESI^+): *m/z* calc. ($C_{18}H_{20}N_6O$) $[M+H]^+$ 337.1771, found 337.1786.

*2.3.3. Synthesis of (Z)-2-(2-amino-6-methylpyrimidin-4-yl)-4-[(4-diethylaminophenyl)-methylidene]-5-methyl-2,4-dihydro-3H-pyrazol-3-one (**6b**)*

Yield: 61%; Mp: 246-248°C. ^1H NMR, δ (ppm) (DMSO-d_6): 1.17 (t, 6H, $\underline{Me}CH_2N$, J = 7.0 Hz), 2.25 (s, 3H, Me), 2.26 (s, 3H, Me), 3.52 (q, 4H, $MeCH_2N$, J = 7.1 Hz), 6.53 (s, 2H, NH_2), 6.83 (d, 2H, ArH, ^3J = 9.3 Hz), 7.25 [s, 1H, C(5)H], 7.52 (s, 1H, H^β), 8.58 (d, 2H, ArH, ^3J = 8.6 Hz). ^{13}C NMR, δ (ppm) (DMSO-d_6): 13.07, 13.59, 19.01, 24.35, 44.64, 56.56, 97.33, 111.5, 118.1, 121.3, 138.5, 148.6 (C^β), 152.3, 152.8, 157.2, 163.6, 164.0, 168.5. IR, ν_{max} (cm^{-1}) (KBr): 1686 ($\nu_{C=O}$), 1632 ($\nu_{C=N}$), 1555 ($\nu_{C=C}$). LC, rt (min): 15.05-15.86. HRMS (ESI^+): *m/z* calc. ($C_{20}H_{24}N_6O$) $[M+H]^+$ 365.2084, found 365.2103.

*2.3.4. Synthesis of (Z)-2-(2-amino-6-methylpyrimidin-4-yl)-4-[(4-methoxyphenyl)-methylidene]-5-methyl-2,4-dihydro-3H-pyrazol-3-one (**6c**)*

Yield: 28%; Mp: 255-257°C. ^1H NMR, δ (ppm) (DMSO-d_6): 2.26 (s, 3H, Me), 2.31 (s, 3H, Me), 3.90 (s, 3H, MeO), 6.60 (s, 2H, NH_2), 7.14 [s, 1H, C(5)H], 7.15 (d, 2H, ArH, ^3J = 2.0 Hz), 7.76 (s, 1H, H^β), 8.65 (d, 2H, ArH, ^3J = 9.0 Hz). ^{13}C NMR, δ (ppm) (DMSO-d_6): 13.65, 24.34, 56.29, 97.46, 114.8, 123.5, 126.5, 137.3, 148.8 (C^β), 153.1, 157.0, 163.4, 163.7, 164.2, 168.7. IR, ν_{max} (cm^{-1}) (KBr): 1698 ($\nu_{C=O}$), 1629 ($\nu_{C=N}$), 1559 ($\nu_{C=N}$). LC, rt (min): 13.63-13.93. HRMS (ESI^+): *m/z* calc. ($C_{17}H_{17}N_5O_2$) $[M+H]^+$ 324.1455, found 324.1458.

*2.3.5. Synthesis of (Z)-2-(2-amino-6-methylpyrimidin-4-yl)-4-[(3,4-dimethoxyphenyl)-methylidene]-5-methyl-2,4-dihydro-3H-pyrazol-3-one (**6d**)*[3]

Yield: 24%; Mp: 240-242°C. ^1H NMR, δ (ppm) (DMSO-d_6): 1.91 (s, 3H, Me, Ac), 2.26 (s, 3H, Me), 2.30 (s, 3H, Me), 3.87 (s, 3H, MeO), 3.91 (s, 3H, MeO), 6.61 (s, 2H, NH_2), 7.14 [s, 1H, C(5)H], 7.18 (d, 1H, ArH, ^3J = 8.6 Hz), 7.74 (s, 1H, H^β), 8.11 (dd, 1H, ArH, ^3J = 8.6 Hz, ^4J = 1.8 Hz), 8.65 (d, 1H, ArH, ^4J = 1.8 Hz). ^{13}C NMR, δ (ppm) (DMSO-d_6): 13.68, 21.48, 24.32, 55.96, 56.32, 97.60, 111.8, 116.4, 123.2, 126.8, 131.2, 148.5 (C^β), 149.4, 153.0, 154.3, 156.9, 163.6, 163.9, 168.8, 172.5. IR, ν_{max} (cm^{-1}) (KBr): 1682 ($\nu_{C=O}$), 1623 ($\nu_{C=N}$), 1659 ($\nu_{C=N}$). LC, rt (min): 13.74-13.94. HRMS (ESI^+): *m/z* calc. ($C_{18}H_{19}N_5O_3$) $[M+H]^+$ 354.1561, found 354.1575.

*2.3.6. Synthesis of (Z)-2-(2-amino-6-methylpyrimidin-4-yl)-4-[(4-hydroxy-3-methoxy-phenyl)methylidene]-5-methyl-2,4-dihydro-3H-pyrazol-3-one (**6e**)*

Yield: 41%; Mp: 285-288°C (dec.). ^1H NMR, δ (ppm) (DMSO-d_6): 2.26 (s, 3H, Me), 2.29 (s, 3H, Me), 3.89 (s, 3H, MeO), 6.61 (s, 2H, NH_2), 6.96 (d, 1H, ArH, ^3J = 8.4 Hz), 7.16 [s, 1H, C(5)H], 7.69 (s, 1H, H^β), 8.04 (dd, 1H, ArH, ^3J = 8.4 Hz, ^4J = 1.8 Hz), 8.66 (d, 1H, ArH, ^4J = 1.7 Hz), 10.65 (bs, 1H, OH). ^{13}C NMR, δ (ppm) (DMSO-d_6): 13.63, 24.18, 56.25, 97.70, 111.2, 115.9, 116.1, 117.7, 122.2, 125.6, 126.5, 129.1, 131.6, 147.8, 148.7 (C^β), 149.6, 153.0, 153.4, 156.9, 163.6, 168.7. IR, ν_{max} (cm^{-1}) (KBr): 1682 ($\nu_{C=O}$), 1644 ($\nu_{C=N}$), 1562 ($\nu_{C=C}$). LC, rt (min): 13.33-13.43. HRMS (ESI^+): *m/z* calc. ($C_{17}H_{17}N_5O_3$) $[M+H]^+$ 340.1404, found 340.1415.

*2.3.7. Synthesis of (Z)-2-(2-amino-6-methylpyrimidin-4-yl)-4-[(4-hydroxy-3-ethoxy-phenyl)methylidene]-5-methyl-2,4-dihydro-3H-pyrazol-3-one (**6f**)*

Yield: 27%; Mp: > 280°C (dec.). ^1H NMR, δ (ppm) (DMSO-d_6): 1.41 (t, 3H, $\underline{Me}CH_2O$, J = 6.9 Hz), 2.26 (s, 3H, Me), 2.29 (s, 3H, Me), 4.14 (q, 2H, $MeCH_2O$, J = 6.9 Hz), 6.60 (s, 2H, NH_2), 6.97 (d, 1H, ArH, ^3J = 8.4 Hz), 7.15 [s, 1H, C(5)H], 7.67 (s, 1H, H^β), 8.03 (dd, 1H, ArH, ^3J = 8.5 Hz, ^4J = 1.8 Hz), 8.62 (d, 1H, ArH, ^4J = 1.7 Hz), 10.53 (bs, 1H, OH). ^{13}C NMR, δ (ppm) (DMSO-d_6): 13.50, 15.12, 24.49, 64.29, 97.58, 116.1, 118.9, 122.0, 125.7, 131.5, 146.8, 149.6 (C^β), 152.9, 153.8, 157.0, 163.6, 163.7, 168.7. IR, ν_{max} (cm^{-1}) (KBr): 1684 ($\nu_{C=O}$), 1614 ($\nu_{C=N}$), 1563 ($\nu_{C=C}$). LC, rt (min): 13.84-14.04. HRMS (ESI^+): *m/z* calc. ($C_{18}H_{19}N_5O_3$) $[M+H]^+$ 354.1561, found 354.1574.

*2.3.8. Procedure for the synthesis of 2-amino-4-chloro-6-methylpyrimidine (**8**)*

A mixture of pyrimidinone **7** (10 g, 80 mmol) and freshly distilled phosphorus oxychloride (50 mL) was heated to 115°C and kept at this temperature until homogenization, which occurred within 20 min. Afterwards, excess of phosphorus oxychloride was distilled off under diminished pressure. The residue was cooled to 5°C and mixed with crushed ice. Then, 25% aqueous ammonia was added to this mixture until pH thereof achieved 8÷9. The suspension thus formed was filtered; the precipitate was washed with water to remove most of inorganic salts, recrystallized from 50% aqueous ethanol and dried at 70°C to a constant weight. Yield: 6.14 g (53%); Mp: 186-188°C (Ref [24] 176.5-181°C, Ref [25] 183-186°C, Ref [26] 182°C).

*2.3.9. Procedure for the synthesis of 2-amino-4-hydrazino-6-methylpyrimidine (**9**)*

A mixture of chloropyrimidine **8** (2.0 g, 14 mmol) and hydrazine hydrate (4.2 g, 84 mmol) was heated at 100°C for 30 min. After cooling to room temperature, the mixture was diluted with water (15 mL), the solid was filtered off, washed with water and dried at 70°C to a constant weight. Yield: 1.75 g (90%); Mp: 234-236°C. Analytical sample was prepared by recrystallization of a small amount of crude compound **9** from water. Mp: 236-238°C (Ref [27] 237-238°C, Ref [28] 240°C).

*2.3.10. Procedure for the synthesis of 2-(2-amino-6-methylpyrimidin-4-yl)-5-methyl-2H-pyrazol-3-ol (**10**)*

To a boiling solution of hydrazinopyrimidine **9** (1 g, 7.2 mmol) in water (40 mL) freshly distilled ethyl acetoacetate (0.94 g, 7.2 mmol) was added at once. The mixture was refluxed for 1 h, and then it was cooled to room temperature. The precipitate formed was filtered off, washed with water, recrystallized from H_2O-AcOH (12:1, v/v) and dried at 70°C to a constant weight. Yield: 1.75 g (59%); Mp: 244-246°C. ^1H NMR, δ (ppm) ($CDCl_3$): 2.26 (s, 3H, Me), 2.41 (s, 3H, Me), 5.06 (s, 2H, NH_2), 5.43 [s, 1H, C(4)H], 7.01 [s, 1H, C(5)H], 12.20 (bs, 1H, OH). ^{13}C NMR, δ (ppm) ($CDCl_3$): 14.72, 24.50, 88.84, 97.18, 151.3, 152.6, 153.1, 157.4, 159.9. IR, ν_{max} (cm^{-1}) (KBr): 3446 (ν_{OH}, ν_{NH2}), 1633 ($\nu_{C=N}$), 1583 ($\nu_{C=C}$). LC, rt (min): 5.26-5.85. HRMS (ESI^+): *m/z* calc. ($C_9H_{11}N_5O$) $[M+H]^+$ 206.1036, found 206.1030.

2.4. Microbiological assay

The target compounds were screened *in vitro* for antimycobacterial activity against a standard strain, *Mycobacterium tuberculosis* $H37R_V$, grown on the Soton medium, which contained 10% of horse serum, and the density of microbial suspension when seeding was $50 \bullet 10^6$ cell/L. Antimycobacterial effect was determined by the serial dilution method. Substances were dissolved in DMSO and titrated in the medium N-1, so that the preparation was contained in separate test tubes with the medium in concentration from 100 to 1.56 μg/mL. The concentrations of the substance in the medium in adjacent test tubes differed by the factor of two. DMSO titrated in the same way as the substrate was utilized for the control. The results were considered after a 72 hours cultivation of the mycobacteria at 37°C.

[3] This compound was isolated as a 1:1 solvate with acetic acid

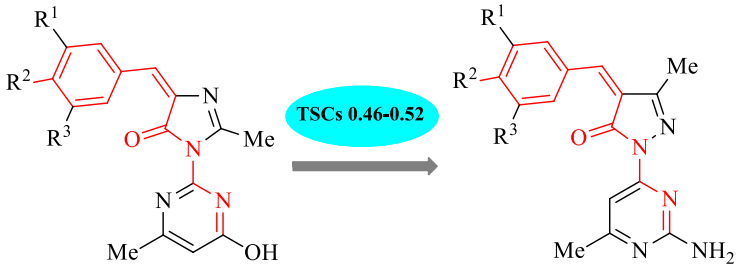

5a-c

5a, $R^1 = R^3 = H$, $R^2 = Me_2N$
5b, $R^1 = R^3 = H$, $R^2 = MeO$
5c, $R^1 = R^2 = R^3 = MeO$

6a-f

6a, $R^1 = R^3 = H$, $R^2 = Me_2N$
6b, $R^1 = R^3 = H$, $R^2 = Et_2N$
6c, $R^1 = R^3 = H$, $R^2 = MeO$
6d, $R^1 = R^2 = MeO$, $R^3 = H$
6e, $R^1 = MeO$, $R^2 = HO$, $R^3 = H$
6f, $R^1 = EtO$, $R^2 = HO$, $R^3 = H$

Fig. 2. HIV-1 RT inhibitors 5a-c and their structural analogues 6a-f (common fragments are marked with red).

2.5. Computational studies

The following online services were used in this work: ChemMine Tools (www.chemminetools.ucr.edu) for calculation of Tanimoto similarity coefficients (TSCs) [29], Way2Drug Predictive Services (www.way2drug.com) for estimation of biological activities [30], Molinspiration Cheminformatics (www.molinspiration.com) for calculation of molecular properties, NMRShiftDB (www.nmrshiftdb.nmr.uni-koeln.de) for ^{13}C NMR spectra simulation [31], Mcule drug discovery platform (www.mcule.com) for molecular docking study [32][4], LiteMol (www.litemol.org) [34], and Protein-Ligand Interaction Profiler (PLIP) (www.projects.biotec.tu-dresden.de) [35] for visualization of the docking study results.

3. Results and discussion

3.1. Design strategy

During a literature survey we turned attention to the very close structural similarity between the Knoevenagel condensation products **4** and 2-R-5-(het)arylmethylidene-3-(4-methyl-pyrimidin-2-yl)-4,5-dihydro-1*H*-imidazol-4-ones (**5**), which emerged as a new class of non-nucleoside type of HIV-1 RT inhibitors. Of them, the compounds bearing a small hydrophobic substituent R, such as methyl group, combined with a bulky aromatic moiety, met with general requirements for the activity [36]. In particular, arylideneimidazolones **5a-c** (Fig. 2) exerted a significant inhibitory effect on the enzyme: when tested at 20 μg/mL, they showed 51-71% inhibition as compared to 100% at the same concentration for nevirapine. In this regard, we evaluated 2-(2-amino-6-methylpyrimidin-4-yl)-4-arylmethylidene-5-methyl-2,4-dihydro-3*H*-pyrazol-3-ones (6a-f) (Fig. 2) *in silico* for their possible anti-HIV properties. This seemed quite reasonable in view of that TSCs for the corresponding pairs of reference arylideneimidazolones 5a-c and compounds 6a-f ranged from 0.46 to 0.52 (Table S3).

Unexpectedly, arylidenepyrazolones **6a-f** demonstrated very low probabilities to be active (P′a < 0.09) against HIV; instead, they proved to possess anti-tubercular (anti-TB) properties with probabilities (P″a) varied from 0.263 to 0.437 (Table 1).

Table 1
The probabilities for compounds 6a-f to be active against HIV (P′a) and TB (P″a).

Tested compound	P′a	P″a
6a	0.079	0.263
6b	0.068	0.344
6c	0.076	0.346
6d	0.077	0.359
6e	0.083	0.408
6f	0.087	0.437

On the one hand, the P″a values indicated that the chance to confirm the predicted activity by *in vitro* experiments was alas not high. On the other hand, these values might be considered as no more than a measure of the structural similarities of compounds **6a-f** and anti-TB drugs known up to date [30]. Be it that way or another, even partial confirmation of the predicted activity may provide an impetus for in-depth study of arylidenepyrazolones **6a-f** as novel[5] potential anti-TB drugs. Indeed, the fact that compounds **6a-f** complied with Lipinski's Rule of Five was a criterion to classify them as drug-like molecules (Table S4).

Some comments should probably be given with regard to the scope of compounds **6a-f** limited by six examples. At the anti-HIV activity prediction step, we aimed to achieve acceptable structural similarities of reference arylideneimidazolones **5a-c** and the target compounds. Later, during the synthesis of arylidenepyrazolones **6a-f**, we came to the conclusion that only electron-donating groups at *para*-position of the aromatic ring facilitated their formation. Besides, some compounds [e.g., halogenated derivatives of compound **6e** (R^3 = Cl, Br)] were excluded from the current research due to their poor solubility in DMSO. This property obviously prevented both spectral characterizations and biological screening of the mentioned derivatives.

3.2. Synthesis

Arylidenepyrazolones **6a-f** were prepared in four-step synthesis outlined in Scheme 1. Compound **10** and its Knoevenagel condensation products **6a-f** were synthesized for the first time.

[4] Along with other docking tools, such as AutoDOCK, GLIDE, GOLD, FlexX, Mcule affords equally reliable and accurate results [33]

[5] In any case, there are no structural analogues of compounds **6a-f** among promising anti-TB pyrazoles and pyrazole-pyrimidine hybrids, which have recently been reviewed [4, 37].

Initially, we carried out the exchange chlorination of commercially available 2-amino-6-methylpyrimidin-4(3*H*)-one (**7**) with a large excess of phosphorus oxychloride to obtain 2-amino-4-chloro-6-methylpyrimidine (**8**). This procedure was successfully modified by replacing the prolonged refluxing of the reaction mixture [24–26] with heating thereof at 115°C until homogenization occurred. Next, chloropyrimidine **8** and 6-fold excess of hydrazine hydrate were kept at 100°C with occasional stirring to afford 2-amino-4-hydrazino-6-methylpyrimidine (**9**). In contrast to the older synthetic protocol [27], we found that the hydrazinolysis of compound **8** required to use no anhydrous hydrazine and could take much less than 2 h to be completed. At the same time, we failed to prepare hydrazinopyrimidine **9** by refluxing the reactants in ethanol as described earlier [28]. Then, the condensation of compound **9** and ethyl acetoacetate in boiling water was performed. The reaction was of remarkable interest as it led to 2-(2-amino-6-methyl-pyrimidin-4-yl)-5-methyl-2*H*-pyrazol-3-ol (**10**) directly, without isolation of the corresponding intermediate ethyl acetoacetate (pyrimidin-4-yl)hydrazone. Moreover, it required no alkaline catalyst to make the above hydrazone undergo the pyrazole ring closure smoothly. Finally, we introduced pyrazol-3-ol **10** into the reaction with aromatic aldehydes bearing electron-donating groups at *para*-position of the ring in glacial acetic acid at 80°C to obtain Knoevenagel condensation products **6a-f**. While acetic acid and DMF allowed the reaction to proceed under homogeneous conditions, other suitable [38] solvents, such as ethanol, acetonitrile and benzene, did not. However, DMF was discarded as the reaction medium to avoid possible [39] aminomethylenation of pyrazol-3-ol **10**. If the aldehydes bore no electron-donating groups, no products of type **6a-f** appear to be formed. For example, the reaction of pyrazol-3-ol **10** with unsubstituted benzaldehyde gave two compounds. Identification of the first one was not possible by even ^{1}H NMR spectroscopy due to extremely poor solubility in common organic solvents, including DMSO, both at room and higher temperatures. ^{1}H NMR spectrum of the second one allowed presuming that it was the crude product of the tandem Knoevenagel-Michael condensation of pyrazol-3-ol **10** with benzaldehyde, 4,4′-(phenylmethanediyl)-bis[2-(2-amino-6-methylpyrimidin-4-yl)-5-methyl-2*H*-pyrazol-3-ol] (**11**). Anyway, the spectrum contained the proton signals, whose chemical shifts, multiplets and integral intensities might correspond to the C-methyl groups attached to the pyrazole and the pyrimidine rings, and the exocyclic methine group (Figure S1).

To explain the formation of methanediylbispyrazol-3-ol **11**, we assumed that the nature of the substituent at *para*-position of the aromatic aldehydes might play a crucial role in stabilization of resulting heterocycles. If the position was occupied with an electron-donating group (EDG) (pathway *a*), the formation of Knoevenagel condensation products **6a-f** took place via adduct **A** (R^2 = EDG) followed by its dehydration. When unsubstituted benzaldehyde was used, structurally related adduct **B** ($R^1 = R^2 = R^3 = H$) was also formed apparently (pathway *b*), but on dehydration it afforded unstable intermediate **C** ($R^1 = R^2 = R^3 = H$). For its stabilization, nucleophilic addition of the second pyrazol-3-ol **10** molecule occurred, giving tandem Knoevenagel-Michael reaction product **11** (Scheme 2).

Noteworthy, a similar reaction course was observed in the case of 2-[6-methyl-2-(methylsulfanyl)pyrimidin-4-yl]-5-methyl-2*H*-pyrazol-3-ol **12**, which, depending on the nature of substituent R^2 in aromatic aldehyde, formed either arylidenepyrazolone **13** or methanediylbispyrazol-3-ol **14** [40].

3.3. Spectral characterizations of arylidenepyrazolones *6a-f*

The structure of arylidenepyrazolones **6a-f** was confirmed by a combination of ^{1}H and ^{13}C NMR spectra, IR spectra, and high resolution mass spectra. In the ^{1}H NMR spectra, the proton signals at δ 2.25-2.30 ppm corresponded to both methyl groups, at δ 6.45-6.61 ppm to NH_2 groups, at δ 7.45-7.74 ppm to the ylidene fragment (H^β), and at δ 6.7-8.6 ppm to aromatic rings. The ^{13}C NMR spectra contained signals, some of which might be attributed to both methyl groups (at δ 13.50-13.68, 24.31-24.49 ppm), C(5) atom (at δ 97.33-97.78 ppm) and aromatic carbons (starting at δ 111 ppm and on).

For accurate assignment of the characteristic C^β atom signal, we performed a series of experiments, such as DEPT-135, {^{1}H-^{13}C}HMQC and {^{1}H-^{13}C}HMBC. For example, of the set of signals in the ^{13}C NMR DEPT-135 spectrum of arylidenepyrazolone **6a**, only four at δ 97.59, 111.9, 138.1, 148.8 ppm might correspond to sp^2 hybridized carbon atoms. On the basis of a joint examination of the complex of correlations in the mentioned heteronuclear spectra (Fig. 3a,b), the latter signal could be unambiguously assigned to C^β atom.

Unfortunately, two signals at δ 157.2 and 163.7 ppm in the ^{13}C NMR spectrum of compound **6a** could not be assigned as reliably as the signal at δ 148.8 ppm even using {^{1}H-^{13}C}HMBC technique. They were supposed to be attributed to C(2) and C(4) atoms, or vice versa, respectively. However, none showed a cross peak with either the C(5) atom proton or an C(6)-methyl proton. This was probably due to the fact that the corresponding coupling constants ^2J(H,C) and ^4J(H,C) were close to zero. Meanwhile, simulation of the ^{13}C NMR spectrum of arylidenepyrazolone **6a** indicated that more downshifted signal (δ 163.7 ppm) might be assigned to C(2) atom.

In the IR spectra of compounds **6a-f**, a strong absorption band was observed at 1684–1698 cm^{-1} attributable to the stretching vibrations of the C=O group conjugated to the exocyclic double bond. Accordingly, less strong absorption bands at 1644-1614 cm^{-1} and at 1563-1555 cm^{-1} might correspond to the stretching vibrations of the C=N and C=C groups, respectively. The high resolution mass spectra contained the peaks of monoprotonated $[M+H]^+$ molecules with the *m/z* values coinciding with the calculated ones.

3.4. Stereochemistry of arylidenepyrazolones *6a-f*

In DMSO-d_6 solution, compounds **6a-f** were found to exist exclusively as (*Z*)-isomers. It clearly follows from comparison of the observed C(5′)-methyl proton signals (δ 2.27 ppm, in average) with the reported ones for (*Z*)-4-(arylethylidene)-5-methyl-2-(pyrimidin-2-yl)-2,4-dihydro-3*H*-pyrazol-3-ones **15**. Otherwise, the C(5′)-methyl proton signals in arylidenepyrazolones **6a-f** would probably be more shielded because of an anisotropic effect of the aryl ring as it took place in the ^{1}H NMR spectra of 4-(diphenylmethylidene)-5-methyl-2-(pyrimidin-2-yl)-2,4-dihydro-3*H*-pyrazol-3-ones **16** (Fig. 4) [41].

In favor of (*Z*)-configuration of compounds **6a-f**, nuclear Overhauser effect (NOE) unequivocally testifies: for example, this effect was readily detected between a C(5′)-methyl proton and H^β atom in the 2D-NOESY ^{1}H NMR spectrum of arylidenepyrazolone **6a**.

3.5. Crystal structure of arylidenepyrazolone *6a*

The crystal structure of compound **6a** was determined using the single crystal X-ray diffraction (XRD) analysis (Fig. 5)[6]. The crystals of arylidenepyrazolone **6a** suitable for X-ray data collection were obtained after slow evaporation of its DMF solution at room temperature. The summaries of crystal data and refinement parameters for compound **6a** monohydrate are given in Table S1.

As it can be seen from Fig. 5, (*Z*)-configuration of compound **6a** did not vary in going from DMSO-d_6 solution to the crystalline

[6] Note that crystal numbering does not obey the IUPAC numbering rules

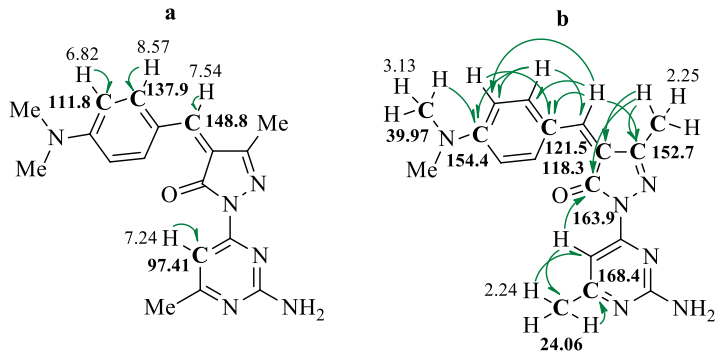

Fig. 3. Correlations and signal assignment in the HMQC (a) and HMBC (b) spectra of compound 6a (carbon atoms and their chemical shifts are marked with bold).

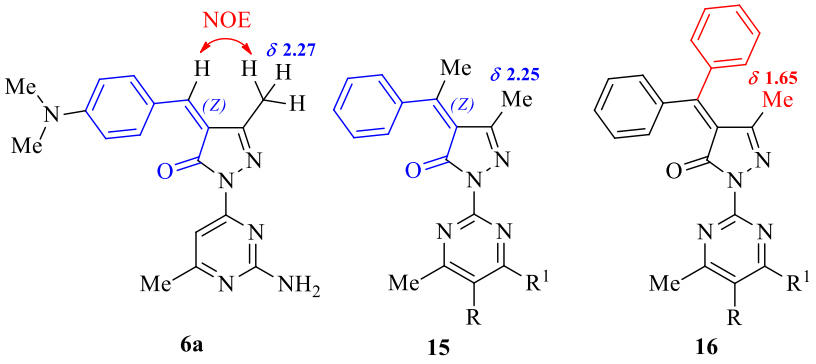

Fig. 4. Chemical shifts of the C(5)-methyl proton signals in compounds 6a, 15 and 16.

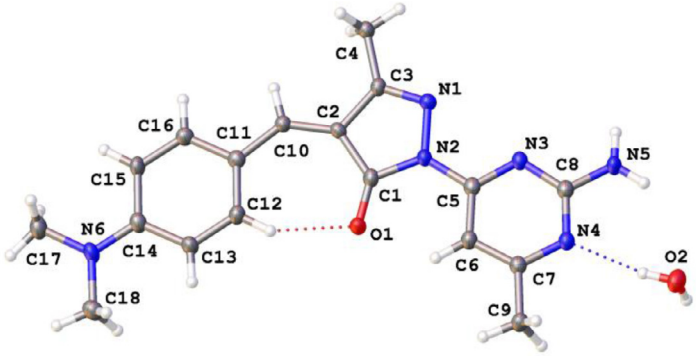

Fig. 5. Crystallographically non-equivalent moiety in the structure of compound 6a. Thermal ellipsoids are shown at the 50% probability level.

Table 2
Intramolecular H-bonds in arylidenepyrazolone **6a.**

BondD–H•••A	Bond lengths (Å) and angles (°)			
	D–H	H•••A	D•••A	D–H•••A
C(6)–H(6)•••O(1)	0.93	2.22	2.828(3)	122.6
C(12)– H(12)•••O(1)	0.93	2.15	2.980(3)	148.6

Table 3
Intermolecular H-bonds in arylidenepyrazolone **6a.**

Bond D–H•••A	Bond lengths (Å) and angles (°)			
	D–H	H•••A	D•••A	D–H•••A
N(5)–H(5)A•••O(2)	0.86	2.63	3.335(3)	139.8
N(5)–H(5)B•••N(3)	0.86	2.16	2.998(3)	166.0
O(2)–H(2)A•••N(4)	0.85	2.03	2.864(3)	167.6
O(2)-H(2)B•••O(1)	0.85	2.16	2.977(3)	161.1
C(17)-H(17)A•••N(1)	0.96	2.69	3.540(4)	147.9

state. The observed structural feature of arylidenepyrazolone **6a** is the formation of two weak intramolecular H-bonds between the H atoms riding on C(6) and C(12), and O(1) atom (Table 2).

In the crystal, arylidenepyrazolone **6a** molecules are arranged in the pseudo-layered complexes (Fig. 6) parallel to (210). Two H_2O molecules are also arranged in the layer, between the compound **6a** molecules. Within the layers, arylidenepyrazolone **6a** molecules are linked through a branchy system of strong and weak hydrogen bonds (Fig. 7, Table 3), involving two H_2O molecules, which include N(5)H•••O(2), N(5)H•••N(3), O(2)H•••N(4), and van der Waals interactions. Layers are interlinked via fewer amounts of less strong H-bonds, which include O(2)H•••O(1), C(17)H•••N(1), and paral-

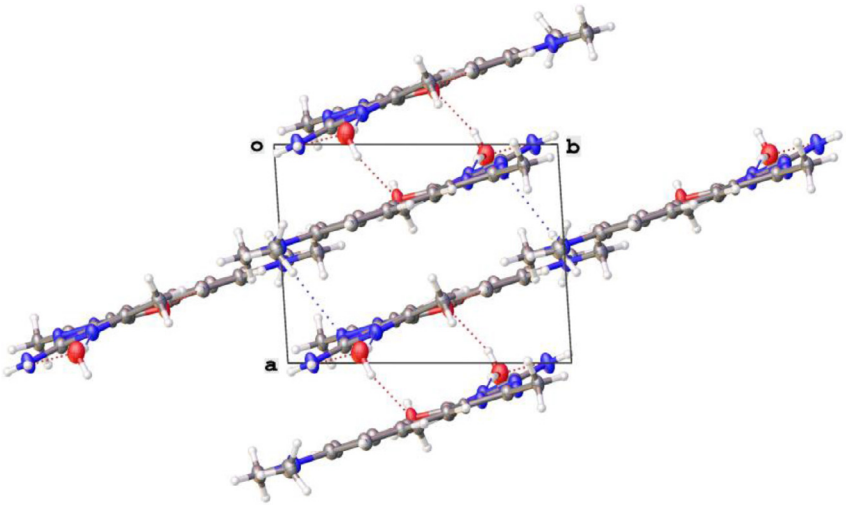

Fig. 6. Packing of compound 6a molecules (view along the [001] and the pseudo-layered complexes). Legend: C atoms = grey, H = white, N = blue, O = red, H-bonds = thin dashed lines.

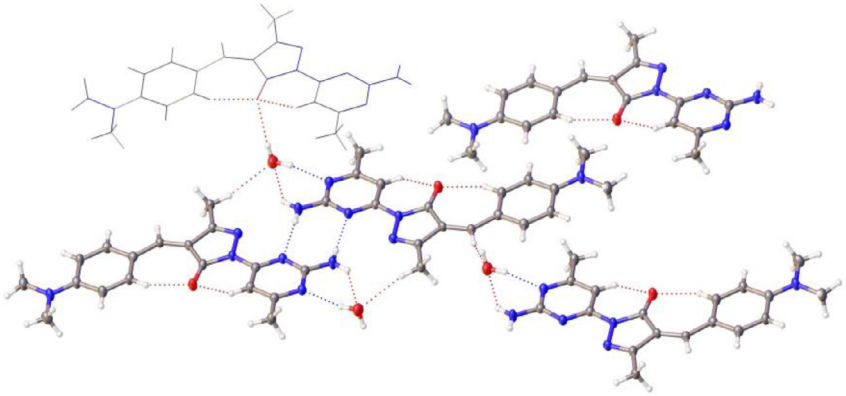

Fig. 7. Arrangement of compound 6a molecules and the H-bonding system within the pseudo-layered complex (the molecule from the neighbor layer is shown as a wire-frame). Legend: see Fig. 6.

lel displaced π-stacking forces between pyrazole [C(1)-N(2)] and aryl [C(11)-C(16)] rings: plane-to-plane normal distance is 3.391(2) Å, plane-to-plane shift is 1.238(5) Å, and plane-to-plane angle is 1.4(1)°.

3.6. Anti-tubercular activity of arylidenepyrazolones ***6a-f***

In vitro biological screening of arylidenepyrazolones **6a-f** showed that some of them possessed an inhibitory effect on *Mycobacterium tuberculosis* $H37R_V$ (*MTub*) growth. This effect was quantified by means of minimal inhibitory concentration (MIC) values. Of all the compounds tested, arylidenepyrazolones **6b, 6d** and **6e** were active against this strain with MIC = 25 (0.068), 50 (0.142) and 25 (0.074) μg/mL (mmol/L), respectively. The MIC values expressed in mmol/L were comparable with the MIC value estimated for first-line anti-TB drug isoniazid (INH) (0.01 mmol/L). Other compounds **6a, 6c** and **6f** possessed no inhibitory effect on *MTub*, when tested at concentrations up to 100 μg/mL.

3.7. Molecular docking study of arylidenepyrazolones ***6b, 6d*** and ***6e***

To clarify a plausible mechanism of anti-TB action of arylidenepyrazolones **6b, 6d** and **6e**, a molecular docking study was performed. Of a great variety of potential targets in *MTub* [42], we focused our attention primarily on the enzymes involved in cell wall construction. This was caused by the fact that INH targets mainly enoyl-[acyl-carrier-protein] reductase (ENR) [43], one of the most important enzymes participating in the biosynthesis of mycolic acids. Apart from ENR enzyme, UDP-galactopyranose mutase (UGM) and alanine dehydrogenase (ALD) were also taken into consideration since they play a prominent role in arabinogalactan and peptidoglycan biosyntheses, respectively [44]. In accordance with modern conception [45], these three biopolymers, mycolic acids, arabinogalactan and peptidoglycan, are the major components of *MTub* cell wall.

As docking scores (DSs) showed, all arylidenepyrazolones **6b, 6d** and **6e** demonstrated the highest binding affinities (DSs $\geq$ 9.3) to UGM enzyme (Table 4).

Table 4
Docking score of compounds **6b**, **6d** and **6e.**

Enzyme	PDB ID	DSs of tested compounds		
		6b	**6d**	**6e**
ENR	2B35	- 8.9	- 8.0	- 8.0
UGM[a]	1V0J	- 9.3	- 10.0	-10.1
ALD	2VG3	- 7.6	- 8.9	- 9.1
SK	2IYV	- 6.9	- 7.2	- 7.9
DHPS1	1EYE	- 6.8	-7.3	-7.1
TK	1GSI	- 7.8	- 8.8	- 7.7

[a] For comparison, DSs for *in vitro* inactive compounds **6a, 6c** and **6f** were equal - 9.7, -10.1 and - 9.1, respectively

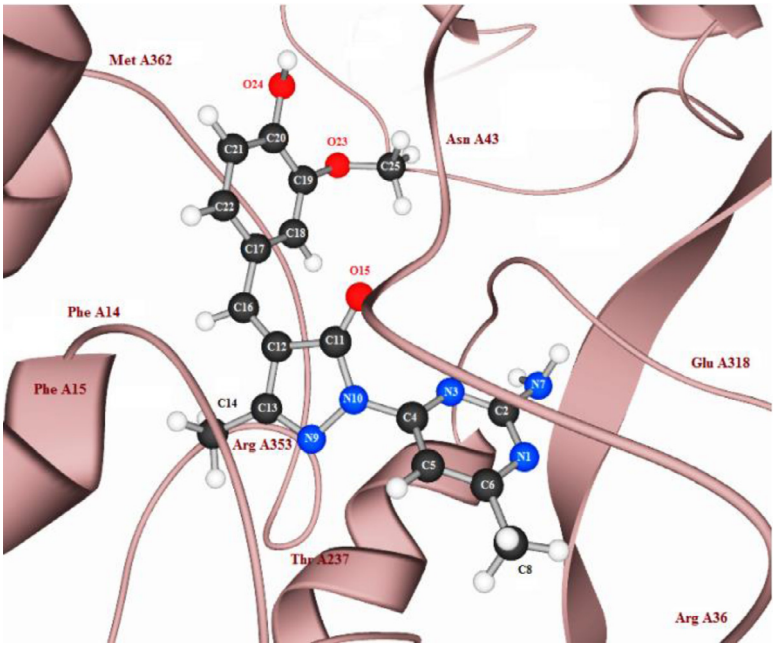

Fig. 8. Docking pose of compound 6e inside UGM enzyme (general view).

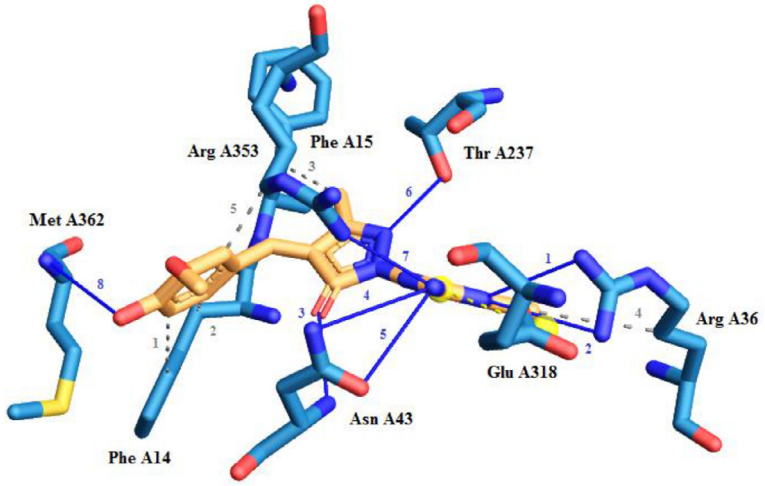

Fig. 9. Interactions of compound 6e with amino acid residues in UGM enzyme (hydrophobic binding interactions are shown with grey dotted, H-bond interactions with dark blue and a salt bridge with yellow dotted).

Inside the enzyme, arylidenepyrazolones **6b, 6d** and **6e** were retained mainly by both hydrophobic and H-bond interactions. In particular, the docking pose of compound **6e** (Fig. 8) revealed[7] a number of hydrophobic interactions with Phe A14, Phe A15, Arg A36 and Arg A353 (Fig. 9, Table 5). In addition to these, a network of H-bond interactions with Arg A36, Asn A43, Thr A237, Arg A353 and Met A362 was observed (Fig. 9, Table 6). Lastly, a salt bridge between guanidine moiety and negative ionizable Glu A318 center at the distance of 4.81 Å was detected.

With regard to other enzymes, such as shikimate kinase (SK), dihydropteroate synthase 1 (DHPS1), and thymidylate kinase (TK) essential for the biosyntheses of some aromatic amino acids (Phe, Tyr, Trp), 7,8-dihydropteroate, and DNA, respectively, compounds **6b, 6d** and **6e** showed lower binding affinities (DSs $\leq$ 8.8) (Table 4).

Table 5
Hydrophobic interactions of compound **6e.**

Index	Amino acid residue	Distance (Å)	Ligand atom	Protein atom
1	Phe A14	3.88	C(21)	C(1) (arom.)
2	Phe A14	3.71	C(22)	C(3) (CH_2)
3	Phe A15	3.34	C(14)	C(3) (CH_2)
4	Arg A36	3.97	C(8)	C(4) (CH_2)
5	Arg A353	3.93	C(18)	C(4) (CH_2)

In most cases, the binding affinities of all arylidenepyrazolones **6a-f** to UGM enzyme were higher than to any other enzyme listed in Table 4. Despite the fact, we believe that only DSs for *in vitro* active compounds appear to be of practical interest. Incidentally, these were noticed to decrease in the same direction

[7] See footnote 6

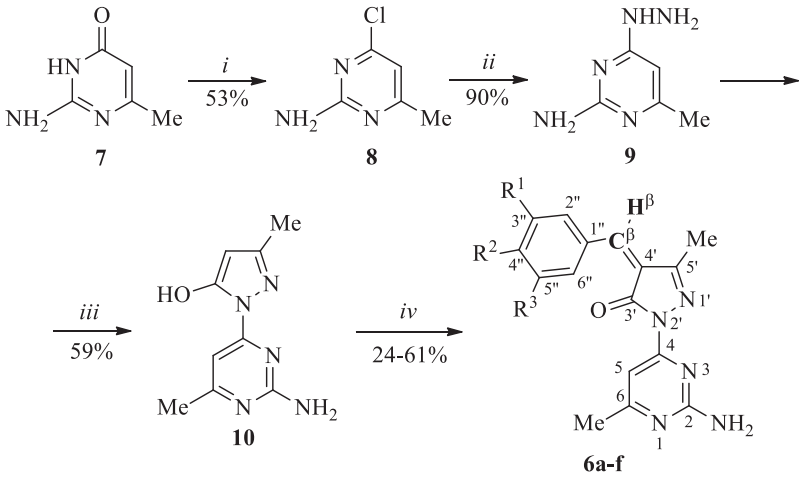

Scheme 1. Synthetic sequence for the preparation of compounds 6a-f Reagents and conditions: *i* – $POCl_3$, 115°C, 20 min; *ii* – $(H_2N)_2 \cdot H_2O$, 80°C, 30 min; *iii* – $AcCH_2COOEt$, H_2O, reflux, 1h; *iv* – 3-R^1-4-R^2-5-$R^3C_6H_2CHO$, AcOH, 80°C, 1 h.

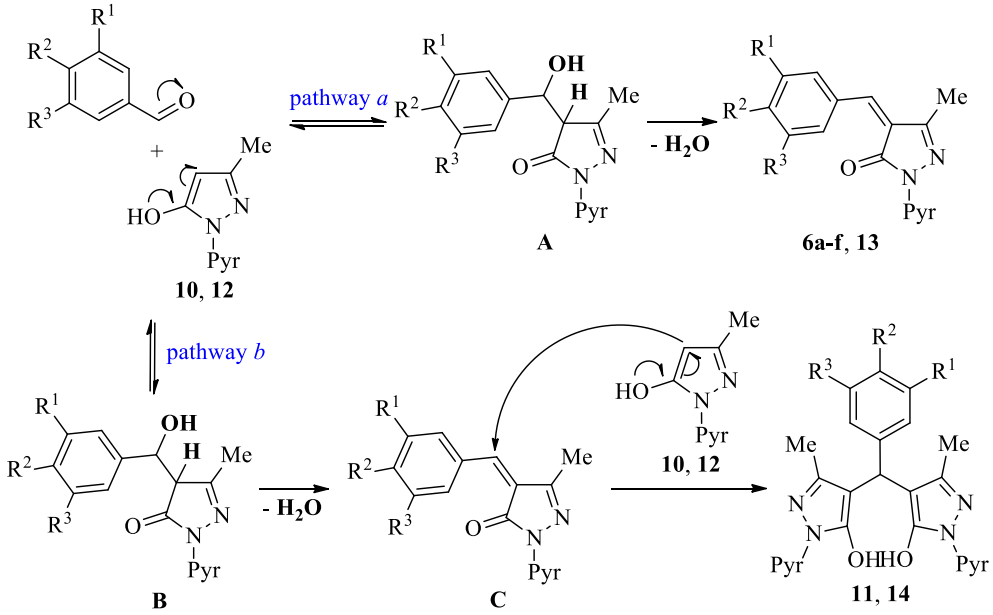

Scheme 2. Proposed mechanism for the formation of arylidenepyrazolones 6a-f, 13 and methylenebispyrazol-3-ols 11, 14 10, Pyr = 2-amino-6-methylpyrimidin-4-yl 11, $R^1 = R^2 = R^3$ = H, Pyr = 2-amino-6-methylpyrimidin-4-yl 12, Pyr = 6-methyl-2-(methylsulfanyl)pyrimidin-4-yl 13, $R^1 = R^3$ = H, $R^2 = Me_2N$, Pyr = 6-methyl-2-(methylsulfanyl)pyrimidin-4-yl 14, $R^1 = R^3$ = H, $R^2 = NO_2$, Pyr = 6-methyl-2-(methylsulfanyl)pyrimidin-4-yl.

Table 6
H-bond interactions of compound **6e.**

Index	Amino acid residue	Donor atom	Acceptor atom	Distance (Å) H-A	D-A
1	Arg A36	HN^+	N(1)	3.31	3.79
2	Arg A36	H_2N^+	N(1)	2.86	3.40
3	Asn A43	H_2N [C(2)]	O(15)	1.93	2.92
4	Asn A43	H_2N [C(4)]	N(7)	3.28	3.82
5	Asn A43	H_2N [N(7)] [a]	O [C(4)] [b]	2.72	3.63
6	Thr A237	HO [C(3)]	N(9)	3.44	3.75
7	Arg A353	HN^+	N(7)	2.11	3.09
8	Met A362	H_2N [C(2)]	O(24)	3.38	3.80

[a] Pyrimidine amino group.
[b] Asn carboxamide group oxygen atom

as both lipophilicities (Log*P*s) and molecular weights (MWs) of arylidenepyrazolones **6b, 6d** and **6e** did (Table S4). Therefore, all these three parameters, DSs, Log*P*s, and MWs, should certainly be taken into account in the forthcoming structural optimization of the mentioned compounds.

4. Conclusions

In summary, 2-(2-amino-6-methylpyrimidin-4-yl)-4-arylmethylidene-2,4-dihydro-3*H*-pyrazol-3-ones **6a-f** were designed as novel potential anti-tubercular agents. For their synthesis, the Knoevenagel condensation of the corresponding pyrazol-3-ol **10** with aromatic aldehydes was performed. However, this reaction was observed to give the desired products only when the aldehydes with electron-donating groups at *para*-position of the ring were used. All compounds **6a-f** were established to exist exclusively as (*Z*)-isomers in DMSO-d_6 solution. In addition, one of them, arylidenepyrazolone **6a**, was shown to retain (*Z*)-configuration in going from the solution to the crystalline state. Of the products synthesized, compounds **6b, 6d** and **6e** were found to exhibit anti-tubercular activity level similar to that of isoniazid.

A plausible mode of action of arylidenepyrazolones **6b, 6d** and **6e** was based on their capability to act as potential inhibitors of UDP-galactopyranose mutase involved in the biosynthesis of arabinogalactan, a building block for the mycobacterial cell wall.

Declaration of Competing Interest

The authors declare no conflict of interest.

CRediT authorship contribution statement

Andrei V. Erkin: Conceptualization, Investigation, Formal analysis, Writing – original draft. **Aleksandra V. Yurieva:** Investigation. **Oleg S. Yuzikhin:** Investigation, Formal analysis. **Vladislav V. Gurzhiy:** Investigation, Formal analysis, Writing – original draft. **Viktor I. Krutikov:** Writing – review & editing, Supervision.

Acknowledgments

We thank the Engineering Centre of the Saint Petersburg State Institute of Technology (Technical University) and the X-ray Diffraction Centre of the Saint Petersburg State University for NMR spectra recording and for XRD analysis, respectively. We also express our gratitude to Anton A. Ivanov, PhD (Pharmaceutical Institute, University of Bonn, Nordrhein-Westfalen, Germany), for a helpful discussion of the paper.

Supplementary materials

Supplementary material associated with this article can be found, in the online version, at doi:10.1016/j.molstruc.2021.130863.

References

[1] K. Sirakawa, 2-(Pyrazol-1-yl)pyrimidine derivatives. US Patent 3,040,047, Jun 19, 1962, Chem. Abstr. 58 (1963) 534.
[2] E. Takabatake, R. Kodama, Y. Tanaka, R. Dohmori, H. Tachizawa, T. Naito, The metabolic fate of 1-(4-methoxy-6-methyl-2-pyrimidinyl)-3-methyl-5-methoxypyrazole (mepirizole, DA-398) in rats and rabbits, Chem. Pharm. Bull. 18 (1970) 1900–1907, doi:10.1248/cpb.18.1900.
[3] M. Ikeda, K. Maruyama, Y. Nobuhara, T. Yamada, S. Okabe, Synthesis and cytoprotective antiulcer activity of 2- or 4-(1*H*-pyrazol-1-yl)pyrimidine derivatives related to mepirizole and dulcerozine, Chem. Pharm. Bull. 44 (1996) 1700–1706, doi:10.1248/cpb.44.1700.
[4] M.F. Khan, M.M. Alam, G. Verma, W. Akhtar, M. Akhter, M. Shaquiquzzaman, The therapeutic voyage of pyrazole and its analogs: a review, Eur. J. Med. Chem. 120 (2016) 170–201, doi:10.1016/j.ejmech.2016.04.077.
[5] A. Adhikari, B. Kalluraya, K.V. Sujith, K. Gouthamchandra, R. Jairam, R. Mahmood, R. Sankolli, Synthesis, characterization and pharmacological study of 4,5-dihydropyrazolines carrying pyrimidine moiety, Eur. J. Med. Chem. 55 (2012) 467–474, doi:10.1016/j.ejmech.2012.07.002.
[6] H. Munier-Lehmann, M. Lucas-Hourani, S. Guillou, O. Helynck, G. Zanghi, A. Noel, F. Tangy, P.-O. Vidalain, Y.L. Janin, Original 2-(3-alkoxy-1*H*-pyrazol-1-yl)pyrimidine derivatives as inhibitors of human dihydroorotate dehydrogenase (DHODH), J. Med. Chem. 58 (2015) 860–877, doi:10.1021/jm501446r.
[7] J.-S. Choi, H. Hwang, S.W. Kim, B.I. Lee, J. Lee, H.-J. Song, J.S. Koh, J.-H. Kim, P.H. Lee, Highly potent and selective pyrazolylpyrimidines as syk kinase inhibitors, Bioorg. Med. Chem. Lett. 25 (2015) 4441–4446, doi:10.1016/j.bmcl.2015.09.011.
[8] M.K. Vekariya, R.H. Vekariya, P.S. Brahmkshatriya, N.S. Shah, Pyrimidine-based pyrazoles as cyclin-dependent kinase-2 inhibitors: design, synthesis, and biological evaluation, Chem. Biol. Drug Des. 92 (2018) 1683–1691, doi:10.1111/cbdd.13334.
[9] M.K. Vekariya, D.B. Patel, P.A. Pandya, R.H. Vekariya, P.U. Shah, D.P. Rajani, N.K. Shah, Novel *N*-thioamide analogues of pyrazolylpyrimidine based piperazine: design, synthesis, characterization, *in silico* molecular docking study and biological evaluation, J. Mol. Struct. 1175 (2019) 551–565, doi:10.1016/j.molstruc.2018.08.018.
[10] M. Hong-Ju, Jian-Hua, X. Xiang-Dong, K. Jing, L. Jian-Hong, Design, synthesis and herbicidal evaluation of novel 4-(1*H*-pyrazol-1-yl)pyrimidine derivatives, Pest. Manag. Sci. 71 (2015) 1189–1196, doi:10.1002/ps.3918.
[11] A.S.T. Lim, I.H. Gilbert, I.M. Vincent, M.P. Barrett, Small polar hits against *S. aureus*: screening, initial hit optimization, and metabolic studies, ACS Omega 4 (2019) 19199–19215, doi:10.1021/acsomega.9b02507.
[12] M. Poirier, J. Pujol-Gimenez, C. Manatschal, S. Bühlmann, A. Embaby, S. Javor, M.A. Hediger, J.-L. Reymond, Pyrazolyl-pyrimidones inhibit the function of human solute carrier protein SLC11A2 (hDMT1) by metal chelation, RSC Med. Chem. 11 (2020) 1023–1031, doi:10.1039/D0MD00085J.
[13] T. Hirayama, K. Nakagawa, Mepirizole. Ger. Offen. 2,237,632, Feb 15, 1973, Chem. Abstr. 78 (1973) 111350.
[14] I. Cristea, Condensation des pyrimidinyl-1-pyrazolones-5 avec des aldehydes aromatiques, Stud. Univ. Babes-Bolyai, Chem. 33 (1988) 61–64.
[15] I. Cristea, I. Panea, Synthesis and stereochemistry of some 4-arylidene-1-pyrimidinyl-2-pyrazolin-5-ones. Part VII, Stud. Univ. Babes-Bolyai, Chem. 40 (1995) 171–175.
[16] I. Panea, I. Cristea, ^{1}H-NMR study of condensation products of 1-(2-pyrimidinyl)-3-methylpyrazolin-5-ones with heterocyclic aldehydes, Stud. Univ. Babes-Bolyai, Chem. 41 (1996) 9–12.
[17] T. Lovasz, C. Paizs, I. Cristea, F.D. Irimie, Synthesis and stereochemistry of some 4-furylidene-1-pyrimidinyl-2-pyrazolin-5-ones, Stud. Univ. Babes-Bolyai, Chem. 43 (1998) 145-148, Chem. Abstr. 137 (2002) 247640.
[18] I. Cristea, M.M. Popovici, M.T. Mendel, I. Silaghi-Dumitrescu, E. Kozma, 1-(Acridin-9′-yl)-pyrazolin-3 and 5-ones. A new class of heterocycles with potential biological activity, Heterocycl. Commun. 5 (1999) 543–548, doi:10.1515/HC.1999.5.6.543.
[19] A.V. Erkin, V.I. Krutikov, M.A. Chubraev, Synthesis of 2-(pyrazol-1-yl)pyrimidine derivatives by cyclocondensation of ethyl acetoacetate (6-methyl-4-oxo-3,4-dihydro-pyrimidin-2-yl)hydrazone with aromatic aldehydes, Russ. J. Gen. Chem. 74 (2004) 423–427, doi:10.1023/B:RUGC.0000030401.30369.4d.
[20] CrysAlisPro, Rigaku Oxford Diffraction, Version 1.171.39.35a (2017).
[21] G.M. Sheldrick, *SHELXT* – integrated space-group and crystal-structure determination, Acta Crystallogr. A71 (2015) 3–8, doi:10.1107/S2053273314026370.
[22] G.M. Sheldrick, Crystal structure refinement with *SHELXL*, Acta Crystallogr C71 (2015) 3–8, doi:10.1107/S2053229614024218.
[23] O.V. Dolomanov, L.J. Bourhis, R.J. Gildea, J.A.K. Howard, H. Puschmann, *OLEX2*: a complete structure solution, refinement and analysis program, J. Appl. Cryst. 42 (2009) 339–341, doi:10.1107/S0021889808042726.
[24] I. Becker, Preparation of pyrimidine derivatives as potential medicinal agents by the reaction of 2-amino-4-chloro-6-methylpyrimidine with primary and secondary amines, J. Heterocyclic Chem. 42 (2005) 1289–1295, doi:10.1002/jhet.5570420707.
[25] B. Aydiner, Z. Seferoğlu, Proton sensitive functional organic fluorescent dyes based on coumarin-imidazo[1,2-*a*]pyrimidine; syntheses, photophysical properties, and investigation of protonation ability, Eur. J. Org. Chem. (2018) 5921–5934, doi:10.1002/ejoc.201800594.
[26] K.T. Santoso, C.-Y. Cheung, K. Hards, G.M. Cook, B.L. Stocker, M.S.M. Timmer, Synthesis and investigation of phtalazinones as antitubercular agents, Chem. Asian J. 14 (2019) 1278–1285, doi:10.1002/asia.201801805.
[27] H. Vanderhaeghe, M. Claesen, Pyrimidines. IV. Hydrazinopyrimidines, Bull. Soc. chim. belg. 68 (1959) 30–46, doi:10.1002/bscb.19590680104.
[28] M. Seada, R.M. Abdel-Rahman, M. El-Behairy, F. Hanafy, Synthesis of some new heterocyclic compounds derived from 2-amino-4-hydrazino-6-substituted pyrimidines, Asian J. Chem. 4 (1992) 604–614.
[29] T.W.H Backman, Y. Cao, T. Girke, ChemMine tools: an online service for analyzing and clustering small molecules, Nucleic Acids Res. 39 (W1) (2011) W486–W491, doi:10.1093/nar/gkr320.
[30] D.A. Filiminov, A.A. Lagunin, T.A. Gloriozova, A.V. Rudik, D.S. Druzhilovskii, P.V. Pogodin, V.V. Poroikov, Prediction of the biological activity spectra of organic compounds using the Pass online web resourse, Chem. Heterocycl. Compd. 50 (2014) 444–457, doi:10.1007/s10593-014-1496-1.
[31] S. Kuhn, N.E. Schlörer, H. Kolshorn, R. Stoll, From chemical shift data through prediction to assignment and NMR LIMS – multiple functionalities of nmrshiftdb2, J. Cheminform. 4 (1) (2012) 52 Suppl., doi:10.1186/1758-2946-4-S1-P52.
[32] R. Kiss, M. Sandor, F.A. Szalai, Http://Mcule.com: a public web service for drug discovery, J. Cheminform. 4 (1) (2012) 17 Suppl., doi:10.1186/1758-2946-4-S1-P17.
[33] D.K. Yadav, R. Rai, R. Pratar, H. Singh, Software and web resources for computer-aided molecular modeling and drug discovery, in: A.G. Mercader, P.R. Duchowics, P.M. Sivakumar (Eds.), Chemometrics Applications and Research: QSAR in Medicinal Chemistry, Apple Academic Press, 2016, pp. 33–99.
[34] D. Sehnal, M. Deshpande, R. Svobodova Vařekova, S. Mir, K. Berka, A. Midlik, L. Pravda, S. Velankar, J. Koča, LiteMol suite: interactive web-based visualization of large-scale macromolecular structure data, Nat. Methods 14 (2017) 1121–1122, doi:10.1038/nmeth.4499.
[35] S. Salentin, S. Schreiber, V.J. Haupt, M.F. Adasme, M. Schroeder, PLIP: fully automated protein-ligand interaction profiler, Nucleic Acid Res. 43 (W1) (2015) W443–W447, doi:10.1093/nar/gkv315.
[36] S.N. Mokale, D.K. Lokwani, D.B. Shinde, Synthesis, in vitro reverse transcriptase inhibitory activity and docking study of some new imidazol-5-one analogs, Med. Chem. Res. 23 (2014) 3752–3764, doi:10.1007/s00044-014-0954-8.
[37] Z. Xu, C. Gao, Q.-C. Ren, X.-F. Song, L.-S. Reng, Z.-S. Lv, Recent advances of pyrazole-containing derivatives as anti-tubercular agents, Eur. J. Med. Chem. 139 (2017) 429–440, doi:10.1016/j.ejmech.2017.07.059.
[38] A. Indrasena, Sd. Riyaz, P.L. Mallipeddi, P. Padmaja, B. Sridhar, P.K. Dubey, Design, synthesis, and biological evaluation of indolylidenepyrazolones as potential anti-bacterial agents, Tetrahedron Lett. 55 (2014) 5014–5018, doi:10.1016/j.tetlet.2014.05.131.

[39] D. Castagnolo, F. Manetti, M. Radi, B. Bechi, M. Pagano, A. De Logu, R. Meleddu, M. Saddi, M. Botta, Synthesis, biological evaluation, and SAR study of novel pyrazole analogues as inhibitors of Mycobacterium tuberculosis: Part 2. Synthesis of rigid pyrazolones, Bioorg. Med. Chem. 17 (2009) 5716–5721, doi:10.1016/j.bmc.2009.05.058.
[40] A.V. Erkin, V.I. Krutikov, 1-(Pyrimidin-4-yl)pyrazol-5(4*H*)-one derivatives. I. Synthesis of 3-methyl-1-(6-methyl-2-methylsulfanylpyrimidin-4-yl)pyrazol-5-ol and specifity of its Knoevenagel reaction, Russ. J. Gen. Chem. 81 (2011) 392–396, doi:10.1134/S1070363211020186.
[41] I. Cristea, I. Panea, Synthesis and structural study of some 4-(α-arylethylidene)-1-pyrimidyl-2-pyrazolin-5-ones, Heterocycl. Commun. 4 (1998) 139–144, doi:10.1515/HC.1998.4.2/139.
[42] Z.S. Bhat, M.A. Rather, M. Maqbool, Z. Ahmad, Drug targets in Mycobacterium tuberculosis: pitfalls and promises on the horizon, Biomed. Pharmacother. 103 (2018) 1733–1747, doi:10.1016/j.biopha.2018.04.176.
[43] K. Mdluli, R.A. Slayden, Y. Zhu, S. Ramaswamy, X. Pan, D. Mead, D.D. Crane, J.M. Musser, C.E. Barry, Inhibition of a Mycobacterium tuberculosis β-ketoacyl ACP synthase by isoniazid, Science 280 (1998) 1607–1610, doi:10.1126/science.280.5369.1607.
[44] K. Mdluli, M. Spigelman, Novel targets for tuberculosis drug discovery, Curr. Opin. Pharmacol. 6 (2006) 459–467, doi:10.1016/j.coph.2006.06.004.
[45] Z.S. Bhat, M.A. Rather, M. Maqbool, H.U. Lah, S.K. Yousuf, Z. Ahmad, Cell wall: a versatile fountain of drug targets in Mycobacterium tuberculosis, Biomed. Pharmacother. 95 (2017) 1520–1534, doi:10.1016/j.biopha.2017.09.036.